On-demand generation of soliton molecules through evolutionary algorithm optimization

J. Girardot, A. Coillet, M. Nafa, F. Billard, E. Hertz, Philippe Grelu

On-demand generation of soliton molecules through evolutionary algorithm optimization

J. Girardot, A. Coillet, M. Nafa, F. Billard, E. Hertz, Philippe Grelu

On-demand generation of soliton molecules through evolutionary algorithm optimization

J. GIRARDOT, A. COILLET, M. NAFA, F. BILLARD, E. HERTZ, AND PH. GRELU*

Laboratoire ICB UMR 6303 CNRS, Université Bourgogne – Franche-Comté, 9 av. Savary, F-21000 Dijon, France
**Corresponding author: philippe.grelu@u-bourgogne.fr*

Received XX Month XXXX; revised XX Month, XXXX; accepted XX Month XXXX; posted XX Month XXXX (Doc. ID XXXXX); published XX Month XXXX

Combining evolutionary algorithm optimization with ultrafast fiber laser technology, we report on the self-generation of stable 2-soliton molecules with controllable temporal separations. A fiber laser setup including an adjustable virtual saturable absorber through nonlinear polarization evolution and an intracavity pulse shaper are used to generate 2-soliton molecules with a user-defined 3 ps to 8 ps internal delay.

Mode-locked fiber lasers constitute a mature technology for numerous applicative fields such as material processing, medicine, sensing, and spectroscopy, with the promise of a steerable source endowed with high beam quality, fired from a compact and cost-effective device [1]. In practice, commercial mode-locked fiber lasers offer a limited pulse output versatility, contrasting with the large range of accessible regimes obtained in labs within most laser architectures [2,3]. One main reason is that shifting from one regime to another usually involves a tedious manual adjustment of the cavity parameters. This is rooted into the complexity of nonlinear laser dynamics, which precludes establishing an analytical relationship between the output pulse profile and the set of cavity parameters. That complexity is exacerbated in multi-pulse regimes, such as in soliton molecules, which are ruled by specific dissipative soliton attractors whose domains of existence are limited in the space of laser parameters and subjected to large hysteretic behaviors [2,4].

In recent years, significant efforts led to self-generation of laser regimes combining a computer control of accessible cavity parameters and the use of a feedback loop fed from measured laser output features. An important step involving artificial intelligence in that process was achieved in 2015, with the implementation of evolutionary algorithms to control the cavity's degrees of freedom according to the user's pre-defined objective [5]. In practice, using nonlinear polarization evolution (NPE) in optical fibers combined with polarization discrimination makes a convenient way to yield an adjustable nonlinear transfer function steered by polarization tuning elements [6]. Successive experimental works have demonstrated the effectiveness of fiber lasers interfaced with genetic or evolutionary algorithm optimization to reach ultrafast regimes of specific interest. In such strategies, optimization is based on a merit score obtained from the measurement of output features such as second-harmonic conversion [5], radiofrequency spectrum [7], optical spectrum and/or optical autocorrelation [8,9]. In a multi-objective optimization, several features are combined [9]. Recently, dispersive Fourier transform (DFT) measurements were used to build multi-objectives optimizations originating from a single oscilloscope [10]. While previous developments tackled a low number of degrees of freedom and targeted the generation of single pulse dynamics, in this Letter, we extend the potential of the evolutionary algorithm approach to the generation of 2-soliton molecules of controllable temporal separation. This is performed through an increase of the number of accessible intracavity parameters, via a computer-controlled free-space pulse shaper allowing to manipulate the spectral transmission of the cavity [11].

An evolutionary algorithm makes a population of "individuals" to evolve so as to optimize a user-defined objective, or merit function [12]. In our context, an individual is a laser regime associated with a given setting of the adjustable parameters of the cavity. These parameters are used as genes of the algorithm. Each individual is tested and ranked through the merit function. Thus, the best individuals are selected as parents of the next generation, and a new population of children is created by crossover and

mutation of their genes, keeping a constant population size. The procedure is iterated until convergence of the merit score within a given maximum number of generations. The optimized laser regime is then fully characterized and compared to the expected objectives.

The experimental scheme of the ring laser cavity is presented in Fig. 1(a) and comprises two sections. The fiber section includes a 980-nm-pumped two-stage erbium-doped fiber (EDF) amplifier allowing high gain to compensate for the extra losses induced by the pulse shaper (5-dB). A polarization-insensitive optical isolator ensures unidirectional lasing in the C+L telecom band. Short lengths of SMF-28 connect the fiber-integrated components. NPE in the optical fibers followed by polarization discrimination yields a virtual ultrafast saturable absorber for mode-locking operation. The second cavity section comprises in free space a set of 4 liquid crystal retarders (LC 1-4), a polarizing beam splitter (PBS), and a home-made pulse shaper. Each LC has its axis oriented at 45° from its neighbor, with the following range of accessible phase retardances: $0<\varphi_{1,4}<\pi$ and $0<\varphi_{2,3}<2\pi$; such a combination allows a full exploration of the transfer function of the saturable absorber [10]. The pulse shaper, see Fig. 1(b), is a 4-f system composed of 2 gratings (G) with a groove frequency of 600 lines.mm^{-1}, 2 lenses with focal length of 40 cm, and a spatial light modulator (SLM) with a 3.2-cm wide dual mask array of 320 pixels located at the Fourier plane. Owing to a rectangular pixel size of 1.3 cm x 100 µm, we use cylindrical focusing which limits the peak intensity well below the damage threshold of the SLM (4 GW.cm^{-2}) for all accessible laser regimes. The setup yields a spectral resolution of 0.39 nm per pixel, giving a temporal window of ± 21.1 ps [13]. A PBS located at the output of the SLM enables the adjustment of both phase and amplitude for each spectral component.

The laser is operated in a slightly normal averaged-dispersion regime, $\beta_{2,net}$ = 0.03 ps^2, owing to the normal chromatic dispersion of the EDF, $\beta_{2,EDF}$=0.06 ps^2.m^{-1}. The total length of the fiber section is kept within 3 meters to improve the laser stability, such that the fundamental repetition rate of the optical cavity is 40 MHz. We operate in a range of total pump power suitable for the generation of 2-soliton molecules, from 0.8 to 1.2 W. In the following, the total pump power is set to 1 W leading to an average output power around 20 mW in the ultrafast regime. For a complete characterization of the laser output after optimization, we use a fast photodiode plugged on a 6-GHz oscilloscope, an optical spectrum analyzer (OSA) with a resolution of 0.07 nm and an optical autocorrelator based on type-II second-harmonic generation.

From the above experimental configuration, two kinds of adjustable cavity parameters, or genes for the algorithm are distinguished: the 4 LC phase retardances governing the NPE-based nonlinear transmission, and the SLM parameters. Regarding the latter, instead of using all pixels retardances as free parameters, an overall parametric function is used to perform the optimization with a small number of genes.

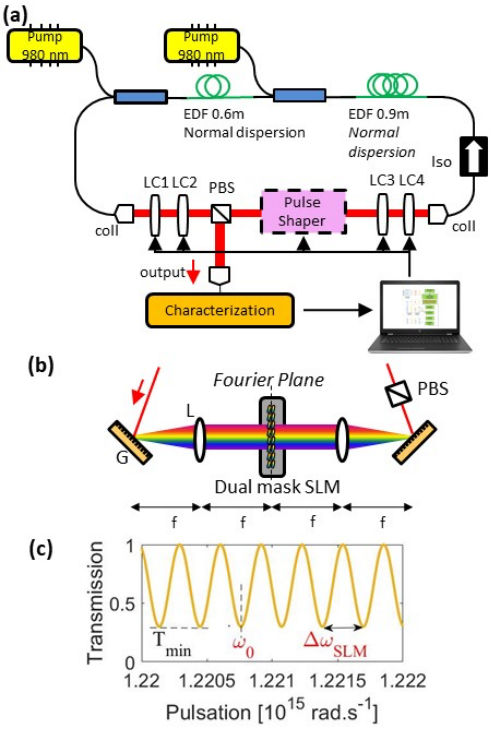

Fig 1. (a) Schematic of the fiber laser setup. EDF: erbium-doped fiber; LC: liquid crystal retarder; PBS: polarizing beam splitter (PBS); coll: collimator. (b) Schematic of the homemade pulse shaper, containing 2 gratings (G), 2 cylindrical lenses (L) and a dual-mask SLM in the Fourier plane. (c) Graph presenting a typical spectral intensity transmission induced by the pulse shaper for the generation of 2-soliton molecules.

The optical spectrum of a stationary 2-soliton molecule has a periodic modulation Δω that is inversely proportional to the temporal separation τ between the 2 solitons: $\tau=2\pi/\Delta\omega$. Therefore, we anticipate controlling the temporal separation within the self-generated soliton molecule by programming a spectral transmission through the SLM of the form: $T(\omega) = 1 - (1 - T_{min})\, cos^2\big((\omega - \omega_0)\,\tau/2\big)$, where ω_0 is the center of the modulation (a dark spectral fringe), and T_{min} is an imposed minimal intensity transmission, see Fig. 1(c). Precisely, we impose a spectral transmittance amplitude $t(\omega) = \sqrt{T(\omega)}$ with the phase masks while applying a constant phase profile. The Fourier transform of such transmittance yields a central peak flanked by smaller peaks separated by the required delay, which will anchor the two solitons and form the molecule from the nonlinear dissipative cavity dynamics over successive cavity roundtrips and corresponding passages through the SLM. We first observed that, starting from a

given soliton molecule regime, it was not possible to switch to another soliton molecule of different separation τ by the mere application of the corresponding spectral modulation, since such a modification generally disrupted the mode locking operation. We attribute this observation to the fact that 2-soliton molecule dynamics relies on specific dissipative soliton attractors [2,14], which depend on the whole set of cavity parameters in a non-trivial way. Therefore, we tested the use of the evolutionary algorithm to find out a new set of cavity parameters encompassing both the need of a suitable saturable absorption with the $\varphi_{1\text{-}4}$ genes and spectral transmission modulation with the $\Delta\omega$ and ω_0 genes, noting that all these genes are interdependent. At first, one could think that $\Delta\omega$ shouldn't be a gene, but a fixed parameter calculated from the user-defined target separation τ. However, we found that freezing completely this parameter reduced considerably the success of soliton molecule generation, illustrating further the complex dependence of soliton molecule attractors on laser cavity parameters. Therefore, the spectral period $\Delta\omega$ was kept as a gene, but its accessible values were constrained to a small range (±5% typically) around the target value $\Delta\omega_{Target}=2\pi/\tau_{Target}$ with τ_{Target} being the user-defined internal pulse separation target.

We then need to design a merit function promoting stable mode locking while discriminating cw emission and unstable regimes such as Q-switched mode-locked regimes. The peak power of the radiofrequency (RF) spectrum at the fundamental repetition frequency of the laser cavity is used to that purpose [5]. At 1-W pump power, the experimental runs showed that by applying the maximum spectral modulation contrast ($T_{min}=0$), mode locking only yielded 2-soliton molecules. It was therefore not necessary to add a merit function part promoting 2-soliton molecules over single pulse mode locking. To sum up, the optimization is now realized over 6 genes ($\varphi_{1\text{-}4}$, $\Delta\omega$ and ω_0): the evolutionary algorithm should find the best set of these 6 parameters to generate the laser regime with the highest RF power, i.e the most stable mode-locked regime with a spectral modulation entailing 2-soliton molecules.

Nevertheless, we found that the success rate of stable 2-soliton molecules generation by the algorithm was enhanced by gradually increasing the contrast of the spectral modulation, from a minimal transmission $T_{min} = 0.3$ at the first generation to $T_{min} = 0$ at the last one. This additional procedure ensured a success rate greater than 90%, compared to 60% obtained with $T_{min} = 0$ fixed from the beginning of the algorithm, and a mere 10% when all spectral genes were frozen. To illustrate our experimental results, let us display a test of laser self-generation of a soliton molecule comprising 2 pulses separated by a pre-determined delay τ = 4.0 ps. The optimization procedure is limited to a maximum of 15 generations, starting from a random population of 140 individuals.

After testing the first generation, the population is reduced to 20 individuals. Each subsequent generation entails a randomly mutated gene for 70% of the children. The optimization curve in Fig. 2(a) displays the maximum and average merit scores obtained for successive generations. The saturation of the maximum score reflects that our merit function only qualifies mode locking stability. Generation after generation, T_{min} is lowered, which imposes a growing constraint on the mode-locked regime, to which the genetic algorithm adapts. At the final generation, a soliton molecule with the required internal separation is obtained. The typical optimization time of the algorithm is 20 minutes. The outcome of such typical optimization leads to the mode-locked regime presented in Fig 2 (b-d).

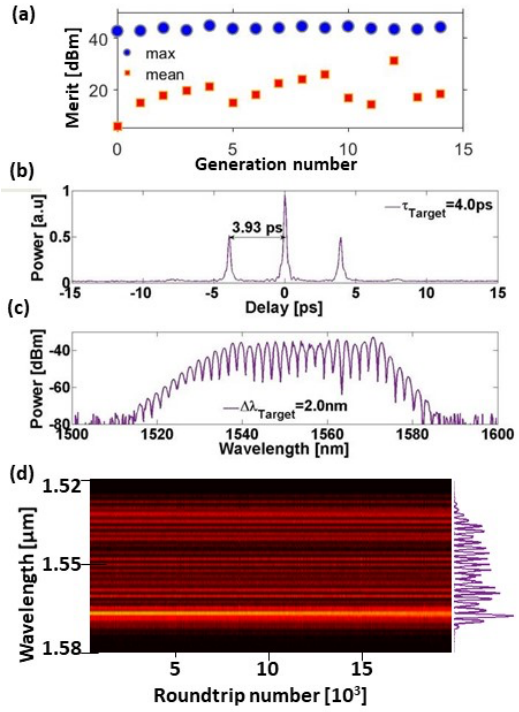

Fig 2. (a) Optimization curve displaying the merit score versus the generation number (see text). Optical characterization of a self-generated soliton molecule obtained after optimization, with a 4-ps separation target: (a) Optical autocorrelation, (b) averaged optical spectrum, (c) DFT trace displaying 20000 consecutive single shot optical spectra, highlighting stationary mode locking.

The 3-peaked autocorrelation trace in Fig. 2(b) is the signature of a molecule consisting of two identical solitons bound together, with lateral peaks having an amplitude half of the central one. The two solitons are separated by a delay of 3.93 ps, which represents a 2% difference with the target. That temporal delay matches the 2.05-nm spectral modulation period shown in Fig 2 (c). Each pulse duration is

estimated to be 150 fs from the autocorrelation trace. Since the emission spans over a broad 40-nm bandwidth, the Time Bandwidth Product (TBP) is 0.75 indicating some frequency chirp. The stationary soliton molecule generation is attested by the DFT trace recorded over 20000 successive roundtrips, shown in Fig 2(d), which presents nearly identical shot-to-shot spectra over a 1-ms lapse of time. We also checked the long-term stability of the soliton molecule regime, which can be maintained for hours. However, subsequent attempts to tune the internal separation within the soliton molecule through the dynamic alteration of the spectral intensity transmission via the wave shaper led to the disruption of the mode-locked regime. Therefore, to modify the temporal separation between the solitons, a new optimization should be performed. We have checked the consistency of this approach by using a spectral modulation period from 1 to 2.5 nm in wavelength, corresponding to temporal delays ranging from 3 to 8 ps. The optimization process was indeed leading to stable 2-soliton molecules in more than 90% of the runs. This is illustrated in Fig. 3, which displays two other optimization results for different targeted delays. The optimal regimes are stable 2-soliton molecules with an internal separation close to the target value. Again, we note the large spectral width (≈40 nm) and high short and long-term stability associated with the ultrafast regimes.

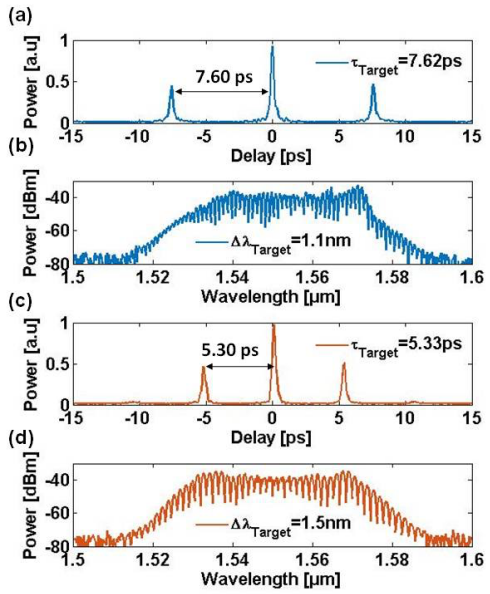

Fig 3. (a) and (c) Optical auto-correlation traces of self-generated soliton molecules obtained after optimization, with internal separation targets τ_{target} = 7.62 ps and 5.33 ps, respectively. (b) and (d): corresponding averaged optical spectra.

In principle, the range of control over the time separation, here from 3 to 8 ps, could be extended. The present upper temporal separation of 8 ps is technically limited by the resolution of the SLM in the Fourier plane, which is 0.3 nm/pixel and impedes imprinting modulations with a period less than ~1 nm, corresponding to 8 ps. The lower boundary at 3 ps seems associated with the dynamics of the interacting chirped pulses featuring pronounced overlap in some sections of the fiber cavity [14]. This boundary is therefore strongly dependent on the cavity architecture and average dispersion.

To summarize, we have illustrated further the potential of evolutionary algorithms to generate complex but well-defined multi-soliton regimes. Using a laser setup combining computer-controlled intracavity polarization and pulse shaping, we generated on demand 2-soliton molecules, with a pre-determined temporal separation from 3 to 8 ps. The prospect of this work is to explore other possible self-generation of on-demand pulse profiles and complex dynamics, moving further the capacities of smart ultrafast lasers [15-17].

Funding. Région Bourgogne Franche-Comté, European Regional Development Fund (FEDER), EUR EiPhi Graduate School (contract ANR-17-EURE-0004), French "Investissements d'Avenir" program: project ISITE-BFC (contract ANR-15-IDEX-0003).

Disclosures. The authors declare no conflicts of interest.

Data availability. Data underlying the results presented in this paper are not publicly available at this time but may be obtained from the authors upon reasonable request.

REFERENCES

1. W. Shi, Q. Fang, X. Zhu, R.A. Norwood, and N. Peyghambarian, Appl. Opt. **53**, 6554 (2014).
2. P. Grelu and N. Akhmediev, Nat. Photon. **6,** 84 (2012).
3. B. Oktem, C. Ülgüdür, and F. Ö. Ilday, Nat. Photon. **4**, 307 (2010).
4. P. Grelu and J.M. Soto-Crespo, Lect. Notes Phys. **751**, 137 (2008).
5. U. Andral, R. Si Fodil, F. Amrani, F. Billard, E. Hertz, and Ph. Grelu, Optica **2**, 275 (2015).
6. V.Matsas, T.Newson, and M. Zervas, Opt. Commun **92**, 61 (1992).
7. U. Andral, R. Si Fodil, F. Amrani, F. Billard, E. Hertz, and Ph. Grelu, J. Opt. Soc. Amer. B **33**, 825 (2016).
8. D. G.Winters, M.S. Kirchner, S.J. Backus, and H.C. Kapteyn, Opt. Express **25**, 33216 (2017).
9. R. I. Woodward and E. J. R. Kelleher, Sci. Rep. **6**, 37616 (2016); Opt. Lett. **42**, 2952 (2017).
10. J. Girardot, F. Billard, A. Coillet, E. Hertz, and Ph. Grelu., IEEE J. Sel. Topics in Quantum Electron. **5**, 1100108 (2020).
11. R. Iegorov, T. Teamir, G. Makey, and F. Ö. Ilday, Optica **3**, 1312 (2016).
12. H.-P. Schwefel, Evolution and Optimum Seeking (Wiley, 1995).
13. E. Hertz, F. Billard, G. Karras, P. Béjot, B. Lavorel, and O. Faucher, Opt. Express **24**, 27702 (2016).
14. Ph. Grelu, J. Béal, and J.M. Soto-Crespo, Opt. Express **11**, 2238 (2003).
15. G. Pu, L. Yi, L. Zhang, and W. Hu, Optica **6**, 362 (2019).
16. G. Genty, L. Salmela, J.M. Dudley, D. Brunner, A. Kokhanovskiy, S. Kobtsev, and S.K. Turitsyn, Nat. Photonics **15**, 91 (2021)
17. T. Baumeister, S. L. Brunton, and J. N. Kutz, J. Opt. Soc. Amer. B **35**, 617 (2018).

REFERENCES with titles

[1] W. Shi, Q. Fang, X. Zhu, R.A. Norwood, and N. Peyghambarian, *Fiber lasers and their applications [Invited]*, Appl. Opt. **53**, 6554 (2014).

[2] P. Grelu and N. Akhmediev, *Dissipative solitons for mode-locked lasers,* Nat. Photon. **6,** 84 (2012).

[3] B. Oktem, C. Ülgüdür, and F. Ö. Ilday, *Soliton-similariton fibre laser,* Nat. Photon. **4**, 307 (2010).

[4] P. Grelu and J.M. Soto-Crespo, *Temporal solitons molecules in mode-locked lasers: collisions, pulsations and vibrations,* in Dissipative solitons: from optics to biology and medicine, N. Akhmediev and A. Ankiewicz Eds, Lect. Notes Phys. **751**, 137 (2008).

[5] U. Andral, R. Si Fodil, F. Amrani, F. Billard, E. Hertz, and Ph. Grelu, *Fiber laser mode locked through an evolutionary algorithm*, Optica **2**, 275 (2015).

[6] V.Matsas, T.Newson, and M. Zervas, *Self-starting passively mode-locked fibre ring laser exploiting nonlinear polarisation switching*, Opt. Commun **92**, 61 (1992).

[7] U. Andral, J. Buguet, R. Si Fodil, F. Amrani, F. Billard, E. Hertz, and Ph. Grelu, *Toward an autosetting mode-locked fiber laser cavity*, J. Opt. Soc. Amer. B **33**, 825 (2016).

[8] D. G.Winters, M.S. Kirchner, S.J. Backus, and H.C. Kapteyn, *Electronic initiation and optimization of nonlinear polarization evolution mode-lockingin a fiber laser,* Opt. Express **25**, 33216 (2017).

[9] R. I. Woodward and E. J. R. Kelleher, *Towards 'smart lasers': self-optimisation of an ultrafast pulse source using a genetic algorithm*, Sci. Rep. **6**, 37616 (2016); *Genetic algorithm-based control of birefringent filtering for self-tuning, self-pulsing fiber lasers*, Opt. Lett. **42**, 2952 (2017).

[10] J. Girardot, F. Billard, A. Coillet, E. Hertz, and Ph. Grelu, *Autosetting Mode-Locked Laser Using an Evolutionary Algorithm and Time-Stretch Spectral Characterization*, IEEE J. Sel. Topics in Quantum Electron. **5**, 1100108 (2020).

[11] R. Iegorov, T. Teamir, G. Makey, and F. Ö. Ilday, *Direct control of mode-locking states of a fiber laser*, Optica **3**, 1312 (2016).

[12] H.-P. Schwefel, Evolution and Optimum Seeking (Wiley, 1995).

[13] E. Hertz, F. Billard, G. Karras, P. Béjot, B. Lavorel, and O. Faucher, *Shaping of ultraviolet femtosecond laser pulses by Fourier domain harmonic generation* Opt. Express **24**, 27702 (2016).

[14] Ph. Grelu, J. Béal, and J.M. Soto-Crespo, *Soliton pairs in a fiber laser: from anomalous to normal average dispersion regime,* Opt. Express **11**, 2238 (2003).

[15] G. Pu, L. Yi, L. Zhang, and W. Hu, *Intelligent programmable mode-locked fiber laser with a human-like algorithm,* Optica **6**, 362 (2019).

[16] G. Genty, L. Salmela, J.M. Dudley, D. Brunner, A. Kokhanovskiy, S. Kobtsev, and S.K. Turitsyn, *Machine learning and applications in ultrafast photonics,* Nat. Photonics **15**, 91 (2021).

[17] T. Baumeister, S. L. Brunton, and J. N. Kutz, *Deep learning and model predictive control for self-tuning mode-locked lasers,* J. Opt. Soc. Amer. B **35**, 617 (2018).